Ore Geology Reviews 101 (2018) 960–965

Contents lists available at ScienceDirect

Ore Geology Reviews

journal homepage: www.elsevier.com/locate/oregeorev

Fluid mixing during late-stage Carlin-type mineralization in the Getchell and Twin Creeks deposits, Nevada

John A. Groff

Department of Earth and Environmental Sciences, New Mexico Institute of Mining and Technology, 801 Leroy Place, Socorro, NM 87801, United States

ARTICLE INFO

Keywords:
Late-stage mineralization
Carlin-type gold deposits
Nevada
Stable isotopes

ABSTRACT

A stable isotope study of orpiment–realgar–calcite–stibnite mineralization in the Getchell and Twin Creeks deposits, Nevada was undertaken to determine the origin(s) of Late-stage fluids. Samples of orpiment have δD values of −48.4‰ to −90.5‰ and $\delta^{34}S$ values of 0.3–2.2‰, which are indicative of a magmatic source. Whereas samples of realgar have δD values of −129.1‰ to −139.7‰ that are indicative of meteoric water and $\delta^{34}S$ values of 4.2–4.9‰, similar to pre-ore/diagenetic pyrite. The δD and $\delta^{13}C$ data of calcite plot to form a mixing trend between fluids with magmatic and meteoric sources. Fluid mixing and wall-rock interaction is supported by the distribution of data in a δD and $\delta^{18}O_{H2O}$ plot for calcite. Additional evidence of fluid mixing is provided by δD values of −55.4‰ to −137.9‰ for stibnite.

These data document how a magmatic fluid produced orpiment–Au mineralization, fluid mixing occurred during calcite deposition, and barren realgar formed from a meteoric water.

1. Introduction

An important step to understanding the genesis of Carlin-type deposits in Nevada was establishing a clear connection between mineralization and Eocene igneous activity, based on age data and geologic relationships (Groff et al., 1997; Ressel et al., 2000; Tretbar et al., 2000; Ressel and Henry, 2006). In this context, genetic models proposed that delamination during subduction of the Farallon Plate generated magmas that assimilated enriched crust, scavenged metals from country rocks, and potentially exsolved an Au–Cu enriched vapor phase at shallow depths to form Carlin-type Au deposits (Cline et al., 2005; Muntean et al., 2011).

The temporal and spatial association of Carlin-type Au deposits with centers of Eocene igneous activity provides strong support of a genetic association. However, fluid inclusion microthermometric and O–H isotope data do not identify a magmatic fluid in many deposits. Tertiary meteoric water dominated the hydrothermal systems that formed the Carlin and Meikle deposits (Fig. 1; Radtke et al., 1980; Emsbo et al., 2003), whereas data for the Deep Star deposit (Fig. 1) only provide evidence for a magmatic fluid at the core of the orebody (Heitt et al., 2003). An absence of Eocene igneous rocks along the Getchell trend (Fig. 1) creates additional uncertainty as to whether Eocene igneous activity served as the heat engine to drive regional fluid flow or provided fluids, and metals, to form Carlin-type Au deposits.

The purpose of this paper is to present stable isotope data for Late-stage minerals in the Getchell and Twin Creeks deposits (Fig. 1). Analyses of O–H–C isotopes were completed for samples of calcite intergrown with realgar from the Main pit, Getchell mine. Additional H–S isotope data were generated for samples of orpiment, realgar, and stibnite from the Getchell and Twin Creeks mines to determine the origin(s) of mineralizing fluids.

2. Geology and mineralization of the Getchell trend

Cambrian–Ordovician carbonate and clastic rocks, containing intercalated basalts, underwent complex deformation prior to the deposition of Pennsylvanian–Permian carbonate units (Chevillon et al., 2000). These rocks were intruded by Cretaceous dacite porphyry dikes, sills and dikes of granodiorite, and the 92 Ma Osgood Mountains granodiorite stock (Fig. 2; Taylor and O'Neil, 1977). Intrusion of the stock altered host rocks to produce a hornfels–wollastonite skarn at the Getchell mine, whereas widespread illitization of Ordovician basalts occurred in association with Cretaceous igneous activity at the Twin Creeks mine (Taylor and O'Neil, 1977; Hall et al., 2000).

Structural controls on mineralization include faults and folds. The NNW-trending Getchell Fault, which occurs near the eastern flank of the Osgood Mountains Stock (Fig. 2), and NE-trending Turquoise Ridge Fault host significant Au orebodies in the Main pit of the Getchell mine. At the Twin Creeks mine, NE-trending faults also contain ore but a northerly trending overturned anticline is the main host for Au

E-mail address: johnagroff@yahoo.com.

https://doi.org/10.1016/j.oregeorev.2018.08.009
Received 2 May 2018; Received in revised form 2 August 2018; Accepted 7 August 2018
Available online 09 August 2018
0169-1368/

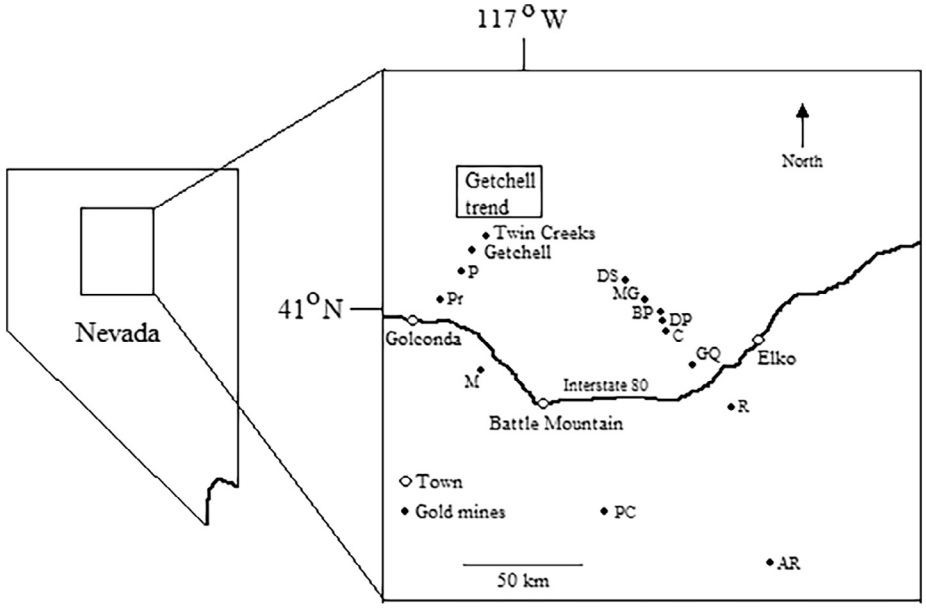

Fig. 1. Location map of the Getchell trend and other Carlin-type Au deposits in north-central Nevada. Abbreviations: BP = Betze–Post, C = Carlin, DP = Deep Star, DS = Dee and Storm, GC = Gold Quarry, M = Marigold, MG = Meikle and Griffin, P = Pinson, PC = Pipeline and Cortez, PR = Preble, and R = Rain.

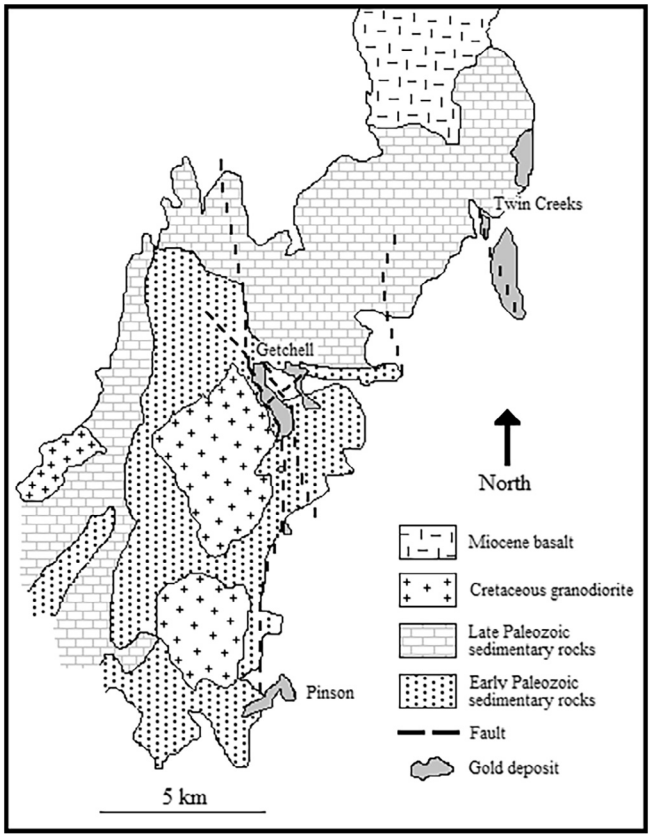

Fig. 2. Geologic map of the Getchell trend after Cline et al. (2005).

Fig. 3. Paragenesis of mineralization for the Getchell and Twin Creeks deposits after Groff (1996) and Shigehiro (1999).

mineralization (Stenger et al., 1998). The deposition of Au in both mines occurred as a result of sulfidation (Stenger et al., 1998; Cline, 2001).

Late-stage mineralization in the Getchell and Twin Creeks deposits occurs as the matrix to breccia containing clasts of Main-stage jasperoid, fracture fillings, and massive veins (up to 1.5 m wide). The mineral assemblage consists of orpiment–realgar–pyrite–stibnite–calcite–gold–quartz ± fluorite and adularia (Fig. 3). These minerals are macroscopic and 1 cm crystals of orpiment, realgar, calcite, and stibnite are common.

Paragenetic relationships indicate that the deposition of orpiment; then calcite and realgar was overlapping and continuous (Fig. 3). Calcite and realgar occur along cleavage planes in orpiment or as open-space fillings around orpiment crystals. The orientation of realgar crystals in calcite is crystallographically controlled and calcite veins can have a selvage of realgar that extends into fractured wall rocks. Gold is associated with orpiment based on assays of mineral separates from the Getchell mine (Groff, 1996) and SEM element mapping of samples from the Twin Creeks mine, which identified finely disseminated auriferous pyrite in orpiment (E.I. Bloomstein, pers. commun.,1995).

Stibnite occurs with different mineral assemblages (Fig. 3). Delicate crystals of intergrown stibnite–realgar–pyrite coat surfaces of calcite and orpiment at the Getchell mine. Stibnite veins, containing fine-grained pyrite (~1–2 mm) and quartz, are commonly vuggy but do not have orpiment or calcite as open-space fillings at the Getchell and Twin Creeks mines. Assay data of mineral separates (Groff, 1996) indicate that stibnite–realgar–pyrite mineralization is barren (e.g., sample #12; Appendix 1), whereas gold (up to 10 ppm) is contained in

stibnite–pyrite–quartz ± adularia veins (e.g., CTW33/263 m; Appendix 1).

3. Materials and methods

Late-stage minerals were studied because they are easily identified and occur as coarse-grained crystals, which allowed for the collection of bulk samples. Mineral separates of calcite, orpiment, realgar, stibnite, and pyrite crystals were examined carefully using a binocular microscope to ensure the purity of samples for isotope analyses. Dilute hydrochloric acid and distilled water were used to clean samples. All isotopic measurements were performed on a Finnigan MAT δE mass spectrometer, calibrated with Oztech gas standards, and housed at the New Mexico Institute of Mining and Technology.

3.1. Oxygen, carbon, hydrogen, and sulfur isotopes

Descriptions of samples used for isotope analyses are provided in Appendix 1. Calcite was separated from intergrown realgar crystals and placed in phosphoric acid overnight to generate CO_2 (McCrea, 1950), which was analyzed for calcite carbon and oxygen isotopes. Values of $\delta^{13}C$ are reported as PDB and have an uncertainty of ± 0.1‰. Multiple analyses of the NBS-19 and NBS-20 standards were used to determine an acid fractionation factor that was applied to the oxygen isotope data, which have an uncertainty of ± 0.2‰.

The hydrogen isotopic composition of fluid inclusion liquids was determined by thermal decrepitation of inclusions and conversion of water to hydrogen at temperatures > 750 °C in a uranium furnace. Aliquots of 5–12 g of orpiment and realgar were heated to 300 °C for 30 min, whereas aliquots of 4–8 g of calcite and stibnite were heated to ~500 °C for 30 min. The liberated gases were collected in a series of dry ice/ethylene glycol and liquid nitrogen traps. The conversion of water to hydrogen was facilitated by interaction with spent uranium turnings at 780–790 °C. Hydrogen was moved through the line and collected using a Toeppler pump. The uncertainty of hydrogen isotope measurements is ± 0.4‰.

Sulfide minerals were mixed with cupric oxide and roasted to yield SO_2 gas. Any SO_3 that may have been generated was converted to SO_2 by interaction with hot copper wool. Sulfide samples were run against the sphalerite NBS-123 standard, and values were then converted to CDT. An average $\delta^{34}S$ value of 17.29 ± 0.14‰ was measured for the sphalerite NBS-123 standard relative to the known value of 17.32‰. The sulfur isotope data have an uncertainty of ± 0.1‰.

4. Results

4.1. Orpiment, realgar, stibnite, and diagenetic pyrite

There are narrow ranges in the S–isotope data of orpiment and realgar (Table 1). Four samples of orpiment from the Getchell and Twin Creeks mines have $\delta^{34}S$ values of 1–2.2‰ and 0.3‰, respectively. The $\delta^{34}S$ values of three realgar samples from the Getchell mine are 4.2–4.9‰. As a comparison, coarse-grained (3–4 mm) diagenetic pyrite was obtained from the Ordovician Comus Formation and has a $\delta^{34}S$ value of 5.9‰.

The H–isotope data of orpiment and realgar are distinctly different (Table 1). Orpiment from the Getchell and Twin Creeks mines has δD values of −48.4‰ to −90.5‰ and −88.5‰, respectively. In contrast, realgar from the Getchell mine has δD values of −129.1‰ to −139.7‰.

The H–isotope data of four samples of stibnite span a range comparable to that of orpiment and realgar combined (Table 1). Massive stibnite intergrown with quartz–pyrite–Au mineralization has δD values of −55.4‰ to −103.8‰, whereas stibnite that occurs with barren realgar as coatings on orpiment (sample #12, Getchell mine) has a δD value of −137.9‰.

Table 1
Sulfur and hydrogen isotope data (‰) of orpiment, realgar, stibnite, and diagenetic pyrite from the Getchell trend. NA = not analyzed.

Sample	Mineral	$\delta^{3}4S$	δD	Mine
#10	Orpiment	2.1 ± 0.1	−48.4 ± 0.6	Getchell
70-2/443 m	Orpiment	2.2 ± 0.1	−90.5 ± 0.3	Getchell
#7	Orpiment	1 ± 0.1	−58.1 ± 1.2	Getchell
R881/136 m	Orpiment	0.3 ± 0.1	−88.5 ± 1.2	Twin Creeks
#2	Realgar	4.9 ± 0.1	−132.9 ± 1.1	Getchell
#8	Realgar	4.2 ± 0.1	−139.7 ± 0.5	Getchell
92-205/327 m	Realgar	4.5 ± 0.1	−129.1 ± 0.7	Getchell
#23	Pyrite	5.9 ± 0.1	NA	Getchell
SED229/323 m	Stibnite	NA	−55.4 ± 0.5	Twin Creeks
CTW33/263 m	Stibnite	NA	−101.5 ± 0.4	Twin Creeks
#12	Stibnite	NA	−137.9 ± 0.5	Getchell
92-280/398 m	Stibnite	NA	−103.8 ± 0.3	Getchell

Table 2
Oxygen, carbon, and hydrogen isotope data (‰) of calcite from the Main Pit, Getchell mine. NA = not analyzed.

Sample	$\delta^{18}O$	$\delta^{18}OH2O$	$\delta^{13}C$	δD
NPSTOPE	22.9 ± 0.1	7.8	−6.9 ± 0.1	−90.8 ± 0.5
#10	14.5 ± 0.1	−0.6	−5.6 ± 0.1	−88.4 ± 0.5
#10	15 ± 0.1	−0.1	−5.7 ± 0.1	NA
99-1550	21.9 ± 0.1	6.8	−6.1 ± 0.1	−103.3 ± 0.2
92-65/282 m	6.9 ± 0.1	−8.2	−4.6 ± 0.1	−104.6 ± 0.7
NP782	23.4 ± 0.1	8.3	−5.9 ± 0.1	−117.9 ± 0.5
NP782	23.2 ± 0.1	8.1	−5.8 ± 0.1	−120.5 ± 0.5
UDG	8.2 ± 0.1	−6.9	−4.2 ± 0.1	NA
UDG	7.7 ± 0.1	−7.4	−4.1 ± 0.1	−122.2 ± 1.2
93-314/113 m	23.5 ± 0.1	8.4	−4.2 ± 0.1	−134.4 ± 0.6
93-314/113 m	23.1 ± 0.1	8	−4.3 ± 0.1	NA

4.2. Calcite

The $\delta^{13}C$ values of −4.1‰ to −6.9‰ (Table 2) for seven samples of calcite from the Main pit, Getchell mine have a limited range compared with the O–H isotope data. Values of $\delta^{18}O_{H2O}$ were calculated using the equation of Friedman and O'Neil (1977) and a temperature of 120 °C, based on microthermometric data for primary fluid inclusions in calcite and realgar (Groff, 1996). The $\delta^{18}O_{H2O}$ values are −8.2‰ to 8.4‰, compared with δD data of −88.4‰ to −134.4‰ (Table 2).

5. Discussion

5.1. The origin(s) of fluids that deposited orpiment and realgar

Genetic models that involve ascending melts assimilating enriched crust and scavenging metals from country rocks (Cline et al., 2005; Muntean et al., 2011) would yield a range in $\delta^{34}S$ values of sulfides in Carlin-type Au deposits. However, primary sulfides in mineralized Eocene igneous intrusions at Bingham Canyon, Utah and the Battle Mountain District, Nevada have $\delta^{34}S$ values of approximately zero (Bowman et al., 1987; Hofstra and Cline, 2000). At the Getchell trend, a magmatic source of sulfur could be suggested by orpiment $\delta^{34}S$ values of 0.3–2.2‰ (Table 1). Whereas the $\delta^{34}S$ value of 5.9‰ for diagenetic pyrite at the Getchell mine is similar to the realgar $\delta^{34}S$ data of 4.2–4.9‰ (Table 1).

By presenting the isotope data of orpiment and realgar in a δD vs. $\delta^{34}S$ plot (Fig. 4), different sources for fluids and sulfur are indicated. The data for orpiment form a group that overlap the magmatic water box and magmatic sulfur. In contrast, the data for realgar plot in a tight cluster that falls within the range of Tertiary meteoric water and overlaps $\delta^{34}S$ values of pre-ore/diagenetic pyrite at the Getchell and Twin Creeks mines.

Fluid inclusion microthermometric and quadrupole mass

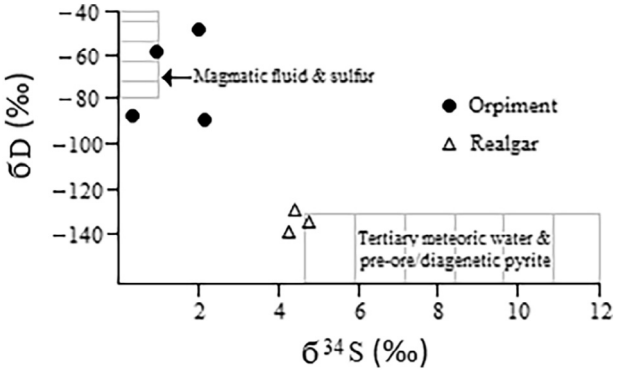

Fig. 4. Plot of δD vs. $\delta^{34}S$ for orpiment and realgar from the Getchell and Twin Creeks deposits. The H–S isotopic composition of magmatic fluids is based on data from Valley et al. (1986). The $\delta^{34}S$ values of pre-ore/diagenetic pyrite are from Osterberg (1990) and the present study. Finally, the δD values of mid-Tertiary meteoric water are based on data from Hofstra et al. (1999) and the measured value of −135‰ for chalcedonic quartz from the Getchell mine (Groff, 1996).

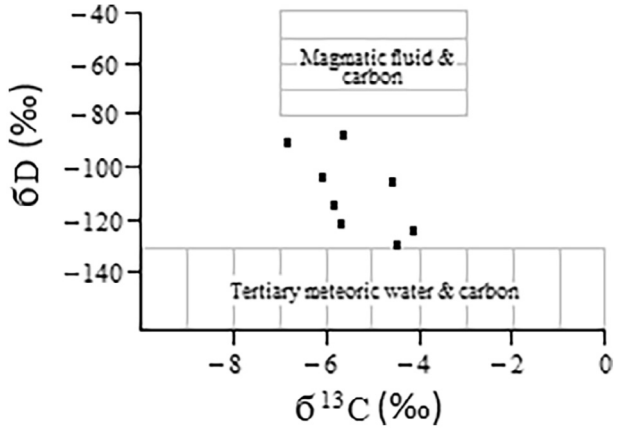

Fig. 5. Plot of δD vs. $\delta^{13}C$ for Late-stage calcite from the Main pit, Getchell mine. The δD and $\delta^{13}C$ (5 ± 2‰) isotopic composition of magmatic fluids is based on data from Valley et al. (1986). The δD and $\delta^{13}C$ values of mid-Tertiary meteoric water are based on data from Groff (1996), Hofstra et al. (1999), and Hofstra and Cline (2000).

spectrometer gas data also record differences between orpiment and realgar. Primary two-phase liquid-dominant inclusions in orpiment have T_h and salinity up to 226 °C and 13.6 wt% NaCl equiv. (Groff, 1996), respectively. Whereas, primary one-phase liquid inclusions in realgar record T_h and salinity of 65 °C and 0 wt% NaCl equiv. (Groff, 1996), respectively. Fluid inclusions in realgar are also gas poor (avg. 0.2 mol%) compared with orpiment (avg. 3.9 mol%) at the Getchell mine (Groff, 1996).

Although distinct fluids formed orpiment and realgar in the Getchell trend, the origin(s) of these minerals in other Carlin-type deposits of Nevada is less clear. Orpiment $\delta^{34}S$ values of 5.3–5.8‰ for Deep Post (Fig. 1; Kesler et al., 2005) and 2.5–12.3‰ for the Alligator Ridge deposit (Fig. 1; Ilchik, 1990) are more similar to data for realgar and pre-ore/diagenetic pyrite from the Getchell trend.

5.2. The origin(s) of fluids that deposited calcite and stibnite

Mineral paragenetic relationships indicate that the deposition of calcite overlapped orpiment–pyrite–Au and younger realgar–pyrite mineralization (Fig. 3). Stable isotope data of calcite from the Main pit, Getchell mine are presented in δD vs. $\delta^{13}C$ and δD vs. $\delta^{18}O_{H2O}$ plots. The δD and $\delta^{13}C$ data of samples define a mixing trend between magmatic and meteoric sources (Fig. 5). Different distributions of data in the δD vs. $\delta^{18}O_{H2O}$ plot record the interaction of a magmatic fluid with wall rocks and mixing between meteoric water and a magmatic fluid (Fig. 6).

Fluid mixing during Late-stage mineralization is also documented by δD values of −55.4‰ to −137.9‰ for stibnite (Table 1). At the Getchell mine, a meteoric water is indicated by the δD value of −137.9‰ for barren stibnite that occurs with realgar and pyrite as a surface coating on orpiment crystals (e.g., sample #12; Appendix 1). In contrast, a magmatic association with Au mineralization is supported by δD values of −55.4‰ to −101.5‰ for ore samples of massive stibnite intergrown with quartz and pyrite from the Getchell and Twin Creeks mines (e.g., SED229/323 m, CTW33/263 m, and 92–280/398 m; Appendix 1). Additional data for stibnite–quartz–pyrite ore include quadrupole mass spectrometer gas analyses of stibnite (avg. 3.5 mol%) and fluid inclusions in quartz that have T_h and salinity up to 253 °C and 6.7 wt% NaCl equiv. (Groff, 1996), respectively.

Therefore, fluids that produced stibnite–pyrite–quartz–Au and orpiment–pyrite–Au mineralization were hotter, more saline, contained higher gas contents, and were deuterium rich compared with barren realgar–pyrite mineralization.

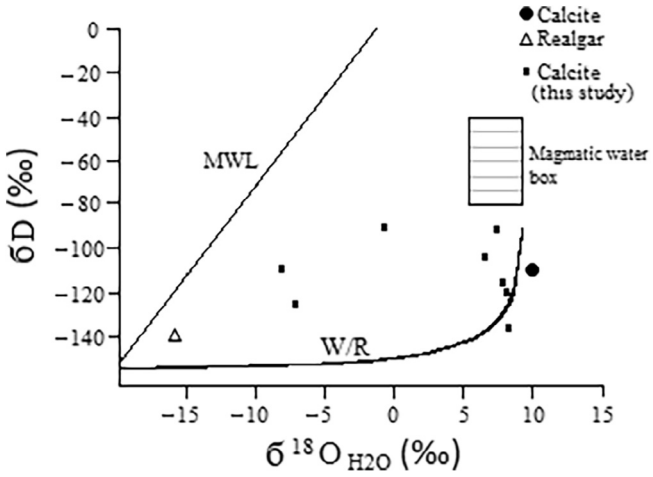

Fig. 6. Plot of δD vs. $\delta^{18}O_{H2O}$ for Late-stage calcite from the Main pit, Getchell mine. The magmatic water box, meteoric water line (MWL), and curve for water–rock interactions (W/R) are included for reference (Valley et al, 1986). Additional data of calcite and realgar from the Turquoise Ridge Deposit are from Shigehiro (1999), with the $\delta^{18}O_{H2O}$ value for calcite recalculated using a temperature of 120 °C to maintain consistency in the presented data.

5.3. Main-stage fluids and evolution of the hydrothermal system

The results of stable isotope studies of Main-stage mineralization at the Getchell and Twin Creeks mines support a magmatic component to the ore fluids. SIMS analyses of ore-stage pyrite from the Getchell mine record $\delta^{34}S$ values of 1–3‰ (Cline et al., 2002). Auriferous jasperoid from the Turquoise Ridge Deposit has δD values of −33‰ to −46‰ (Shigehiro, 1999) and kaolinite, which completely replaces basalt in high-grade ore (18–24 ppm Au) at the Twin Creeks mine, has δD values of −78.8‰ to −89.7‰ (Groff, 1996). There is also evidence of fluid mixing during jasperoid formation based on δD values of −87.3‰ to −153.8‰ for the Getchell mine and −92.1‰ to −206‰ for the Twin Creeks mine (Groff, 1996).

The results of fluid inclusion gas analyses of jasperoid samples confirm a magmatic component to Main-stage ore fluids. Quadrupole mass spectrometer analyses of siliceous ores from deposits of the Getchell trend and the Goldstrike property, Carlin trend (Fig. 1) identified a N_2-rich magmatic fluid characterized by total gas contents of ~10 mol% (Groff, 2018). Element analyses of fluid inclusions in quartz, containing pyrite crystals with Au-rich rims, were used by Large et al.

(2016) to document a magmatic fluid for the Gold Quarry deposit (Fig. 1).

As a magmatic source of ore fluids has not been identified by many stable isotope and fluid inclusion studies (Radtke et al., 1980; Hofstra and Cline, 2000; Emsbo et al., 2003), this could reflect that magmatic fluids were periodically injected into hydrothermal systems dominated by meteoric water and crustal fluids during the formation of Carlin-type deposits. At the Getchell trend, the injection of magmatic fluids is supported by discrete Au events associated with orpiment–pyrite and stibnite–pyrite–quartz mineralization (Fig. 3) that have O–H–S isotope data indicating a magmatic source (Figs. 4–6). In contrast, barren realgar–pyrite mineralization formed from meteoric water based on isotope data (Figs. 4–6) and primary fluid inclusions with T_h of 65 °C and salinity of 0 wt% NaCl equiv. (Groff, 1996). Additional evidence for the injection of auriferous magmatic fluids is provided by Nanosims analyses of pyrite from the Turquoise Ridge deposit that identified distinct textures and chemical zoning to indicate Au deposition occurred as short-lived events within a broader mineralizing system (Barker et al., 2009).

Future research needs to address why magmatic fluids are the most pronounced in Carlin-type deposits of the Getchell trend, where Eocene igneous rocks have not been identified at the surface or through mining and deep drilling.

6. Conclusions

Stable isotope data of Late-stage mineralization in the Getchell and Twin Creeks deposits record the mixing of fluids with magmatic and meteoric sources. Orpiment–Au mineralization formed from a magmatic fluid with δD of −48.4‰ to −90.5‰ and $\delta^{34}S$ of 0.3–2.2‰. The mixing of a magmatic fluid and meteoric water during the deposition of paragenetically younger calcite is indicated by δD of −88.4‰ to −134.4‰, $\delta^{13}C$ of −4.1‰ to −6.9‰, and $\delta^{18}O_{H2O}$ of −8.2‰ to 8.4‰. Finally, barren realgar formed from a meteoric water with δD of −129.1‰ to −139.7‰ and $\delta^{34}S$ of 4.2–4.9‰. These data document how Au, S, and C in Late-stage ore fluids were derived from a magmatic source.

Acknowledgements

The author would like to thank Mr. Richard Nanna (Getchell Gold Corp) and Mr. Dean Peltonen (Santa Fe Pacific Gold Corp) for providing access to collect samples and funding to perform the stable isotope analyses. Constructive comments and thoughtful observations provided by two anonymous reviewers improved the manuscript.

Appendix 1

Descriptions of samples used for stable isotope analyses.

#10, pit sample, Getchell mine. Footwall Fault with orpiment crystals surrounded by intergrown calcite and realgar. The sample contains 21 ppm Au.

70-2/443 m, drill core sample, Getchell mine. Footwall Fault with a 1-cm wide orpiment vein. The sample contains 0.4 ppm Au.

#7, pit sample, Getchell mine. Cretaceous granodiorite cut by orpiment veins (up to 0.5-m wide) in an extension of the Turquoise Ridge Fault. Orpiment crystals are rimmed by realgar. The sample contains 4 ppm Au.

R881/136 m, drill core, Twin Creeks mine. Orpiment vein (~1 m) in HGO ore zone. High-grade ore ≥15 ppm Au.

#2, pit sample, Getchell mine. Getchell Fault with fractures in jasperoid lined by realgar crystals. The sample contains ~5 ppm Au.

#8, pit sample, Getchell mine. Realgar along slip planes in clay gouge and filling open space in a NE-trending fault near the Turquoise Ridge Fault. The sample contains 5.3 ppm Au.

92-205/327 m, drill core, Getchell mine. Breccia in the Footwall Fault with silicified pyrite-rich clasts and a matrix of realgar. The sample contains 19 ppm Au.

#23, pit sample, Getchell mine. Diagenetic pyrite in the Comus Formation near a mineralized NE-trending fault.

SED229/323 m, drill core, Twin Creeks mine. A broken zone cemented by massive stibnite with

intergrown quartz and pyrite. High-grade ore.

CTW33/263 m, drill core, Twin Creeks mine. Adjacent to the NE-trending TC Fault, a 1-m wide stibnite vein with intergrown quartz, pyrite, and 42 Ma adularia. The sample contains 10 ppm Au.

#12, pit sample, Getchell mine. Getchell Fault with realgar and stibnite that occur as coatings on orpiment crystals. The sample contains 5 ppm Au.

92-280/398 m, drill core, Getchell mine. North-trending fault with fracture fillings of intergrown stibnite, pyrite, and quartz. The sample contains 1 ppm Au.

NPSTOPE, pit sample, Getchell mine. Historic drift in the Footwall Fault with a 0.5-m wide vein of intergrown calcite, realgar, and fluorite. High-grade ore zone (> 9 ppm Au).

99-1550, pit sample, Getchell mine. Calcite–realgar veins (up to 7-cm wide) in sericitized and argillized Cretaceous granodiorite cut by the Getchell Fault. The sample contains ~5 ppm Au.

92-65/282 m, drill cuttings, Getchell mine. Footwall Fault with 1-cm wide calcite–realgar veins. The sample contains 2.5 ppm Au.

NP782, pit sample, Getchell mine. Footwall Fault with orpiment, realgar, and calcite along bedding planes. The sample contains ~5 ppm Au.

UDG, drift sample, Getchell mine. Footwall Fault with a 4-cm wide vein of calcite and realgar that cuts argillized ore. Realgar also rims the vein and extends into fractured wall rocks. The sample is in an ore zone containing 9 ppm Au.

93-314/113 m, drill core, Getchell mine. Turquoise Ridge Fault with a 3-cm wide vein of calcite and realgar that cuts silicified and pyritic rocks. Realgar also rims the vein and extends into fractured wall rocks. The sample contains ~2 ppm Au.

Appendix A. Supplementary data

Supplementary data associated with this article can be found, in the online version, at https://doi.org/10.1016/j.oregeorev.2018.08.009.

References

Barker, S.L.L., Hickey, K.A., Cline, J.S., Dipple, G.M., Kilburn, M.R., Vaughan, J.R., Longo, A.A., 2009. Uncloaking invisible gold: use of nanosims to evaluate gold, trace elements, and sulfur isotopes in pyrite from Carlin-type deposits. Econ. Geol. 104, 897–904.

Bowman, J.R., Parry, W.T., Kropp, W.P., Kruer, S.A., 1987. Chemical and isotopic evolution of hydrothermal solutions at Bingham, Utah. Econ. Geol. 82, 395–428.

Chevillon, V., Berentsen, E., Gingrich, M., Howald, W., and Zbinden, E., 2000, Geologic Overview of the Getchell Gold Mine Geology: SEG Guidebook Series, v. 32, pp. 195–205.

Cline, J.S., 2001. The timing of gold and arsenic sulfide mineral deposition at the Getchell Carlin-type gold deposit, north-central Nevada. Econ. Geol. 96, 75–95.

J.S. Cline F.M. Stuart A.H. Hofstra D.R. Tretbar L. Riciputi W. Premo 2002, He, Nd, and Stable isotope constraints on Carlin-type ore fluid components, Getchell NV, USA Geol. Soc. Am. Program Abstracts (gsa.confex.com/gsa/2002AM/final program/abstract_43002.htm).

Cline, J.S., Hofstra, A.H., Muntean, J.L., Tosdale, R.M., Hickey, K.A., 2005. Carlin-type gold deposits in Nevada: critical geologic characteristics and viable Models. Econ. Geol. 100th Anniv. Vol. 451–484.

Emsbo, P., Hofstra, A.H., Lauha, E.A., Griffin, G.L., Hutchinson, R.W., 2003. Origin of high-grade gold ore, source of ore fluid components, and genesis of the meikle and neighboring Carlin-type deposits, Northern Carlin Trend, Nevada. Econ. Geol. 98, 1069–1107.

Friedman, I., and O'Neil, J.R., 1977, Data of Geochemistry: Geol. Surv. Prof. Paper 440-KK, p. 117.

Groff, J.A., 1996. $^{40}Ar/^{39}Ar$ Geochronology of Gold Mineralization and Origin of Auriferous Fluids for the Getchell and Twin Creeks Mines, Humboldt County, Nevada. Unpub. PhD thesis. New Mexico Institute of Mining and Technology, Socorro, pp. 291.

Groff, J.A., 2018. Distinguishing generations of quartz and a distinct gas signature of deep

high-grade Carlin-type gold mineralization using quadrupole mass spectrometry. Ore. Geol. Revs. 95, 518–536.
Groff, J.A., Heizler, M.T., McIntosh, W.C., Norman, D.I., 1997. $^{40}Ar/^{39}Ar$ dating and mineral paragenesis for Carlin-type gold deposits along the Getchell Trend, Nevada: evidence for Cretaceous and Tertiary Gold Mineralization. Econ. Geol. 92, 601–622.
Hall, C.M., Kesler, S.E., Simon, G., Fortuna, J., 2000. Overlapping cretaceous and eocene alteration, twin creeks Carlin-type deposit, Nevada. Econ. Geol. 95, 1739–1752.
Heitt, D.G., Dunbar, W.W., Thompson, T.B., Jackson, R.G., 2003. Geology and geochemistry of the deep star gold deposit, Carlin Trend, Nevada. Econ. Geol. 98, 1107–1131.
Hofstra, A.H., Cline, J.S., 2000. Characteristics and models for Carlin-type gold deposits. Revs. Econ. Geol. 13, 163–220.
Hofstra, A.H., Snee, L.W., Rye, R.O., Folger, H.W., Phinisey, J.D., Loranger, R.J., Dahl, A.R., Naeser, C.W., Stein, H.J., Lewchuk, M., 1999. Age constraints on Jerritt Canyon and other Carlin-Type gold deposits in the Western United States—Relationship to mid-tertiary extension and magmatism. Econ. Geol. 94, 769–802.
Ilchik, R.R., 1990. Geology and geochemistry of the vantage gold deposits alligator ridge-bald mountain mining district, Nevada. Econ. Geol. 85, 50–75.
Kesler, S.E., Riciputi, L.C., Ye, N., 2005. Evidence for a magmatic origin for Carlin-type gold deposits: isotopic composition of sulfur in the Betze-post-screamer deposit, Nevada, USA. Mineral. Deposit. 40, 127–136. https://doi.org/10.1007/s00126-005-0477-9.
Large, S.J.E., Bakker, E.Y.N., Weiss, P., Walle, M., Ressel, M., Heinrich, C.A., 2016. Trace elements in fluid inclusions of sediment-hosted gold deposits indicate a magmatic-hydrothermal origin of the carlin ore trend. Geology 44, 1015–1018.
McCrea, J.M., 1950. The isotopic chemistry of carbonates and a paleotemperature scale. J. Chem. Phys. 18, 849–857.
Muntean, J.L., Cline, J.S., Simon, A.C., Longo, A.A., 2011. Magmatic-hydrothermal origin of Nevada's Carlin-type gold deposits. Nat. Geosci. 6. https://doi.org/10.1038/NGEO1064.
Osterberg, M.W., 1990. Geology and Geochemistry of the Chimney Creek Gold Deposits, Humboldt County, Nevada. Unpub. PhD thesis. Univ. of Arizona, Tucson, pp. 173.
Radtke, A.S., Rye, R.O., Dickson, F.W., 1980. Geology and stable isotope studies of the carlin gold deposit, Nevada. Econ. Geol. 75, 641–672.
Ressel, M.W., Henry, C.D., 2006. Igneous geology of the Carlin trend, Nevada: development of the Eocene plutonic complex and significance for Carlin-type gold deposits. Econ. Geol. 101, 347–383.
Ressel, M.W., Noble, D.C., Henry, C.D., Trudel, W.S., 2000. Dike-hosted ores of the beast deposit and the importance of eocene magmatism in gold mineralization of the Carlin trend, Nevada. Econ. Geol. 95, 1417–1444.
Shigehiro, M., 1999. Mineral Paragenesis and Ore Fluids at the Turquoise Ridge Gold Deposit, Nevada. Unpub. MSc thesis. Univ. of Nevada, Las Vegas, pp. 152.
Stenger, D.P., Kesler, S.E., Peltonen, D.R., Tapper, C.J., 1998. Deposition of gold in Carlin-type deposits; the role of sulfidation and decarbonation at Twin Creeks, Nevada. Econ. Geol. 93, 201–215.
Taylor, B.E., O'Neil, J.R., 1977. Stable isotope studies of metasomatic Ca–Fe–Al–Si Skarns and associated metamorphic and igneous rocks, osgood mountains, Nevada. Contrib. Mineral. Petrol. 63, 1–49.
Tretbar, D., Arehart, G.B., Christensen, J.N., 2000. Dating gold deposition in a Carlin-type gold deposit using Rb/Sr methods on the mineral Galkhaite. Geology 28, 947–950.
Valley, J.W., Taylor Jr, H.P., O'Neil, J.R., 1986. Stable isotopes in high-temperature geological processes: reviews in mineralogy. Mineral. Soc. Am. 16, 570.